

## Adsorption of lead(II) using bioadsorbent prepared from immobilized *Gracilaria corticata* algae: thermodynamics, kinetics and isotherm analysis

Ferdos Kord Mostafapour<sup>a</sup>, Amir Hossein Mahvi<sup>b</sup>, Aram Dokht Khatibi<sup>a</sup>,  
Morteza Khodadadi Saloot<sup>c</sup>, Neghar Mohammadzadeh<sup>d</sup>, Davoud Balarak<sup>a,\*</sup>

<sup>a</sup>Department of Environmental Health, Health Promotion Research Center, Zahedan University of Medical Sciences, Zahedan, Iran, email: dbalarak2@gmail.com (D. Balarak)

<sup>b</sup>Department of Environmental Health Engineering, School of Public Health, Tehran University of Medical Sciences, Tehran, Iran

<sup>c</sup>Department of Environmental Engineering, Faculty of Natural Resources and Environment, Science and Research Branch, Islamic Azad University, Tehran, Iran

<sup>d</sup>Student Research Committee, Zahedan University of Medical Sciences, Zahedan, Iran

Received 14 January 2022; Accepted 20 May 2022

### ABSTRACT

This work focuses on the removal of lead using immobilized *Gracilaria corticata* (immobilized-GC) algal based bioadsorbent. To characterize the surface morphology of the adsorbent by various analytical techniques such as scanning electron microscopy, energy-dispersive X-ray spectroscopy, Fourier transform infrared spectroscopy; the Brunauer–Emmett–Teller and Barrett–Joyner–Halenda analysis were performed. The effect of different parameters was investigated in batch experiments. For the treatment of a Pb(II) solution at 25 mg/L, the removal efficiency of 99.1% was achieved using 1 g/L adsorbent at a mixing time of 75 min and pH of 6 during the adsorption process. Thermodynamics analyses indicate that the Pb(II) sorption on immobilized-GC is feasible, spontaneous, and endothermic with enthalpy and entropy equal to 52.01 kJ/mol and 0.185 kJ/mol K, respectively. Kinetic studies revealed that the adsorption process follows pseudo-second-order due to the higher regression coefficient and lower error coefficient. The adsorption isotherms of Pb(II) were also compared with popular models, and it was found that the Pb(II) uptake was well-described by the Langmuir model with maximum adsorption capacities of 89.1, 98.3, 108.2, and 122.1 mg/g at 20°C, 30°C, 40°C, and 50°C, respectively.

**Keywords:** Immobilized *Gracilaria corticata*; Lead; Adsorption process; Thermodynamic

### 1. Introduction

Contamination of aquatic environments by heavy metals is one of the major environmental challenges because of their flexibility, aggregation, persistence, and non-biodegradable nature [1,2]. Some of the toxic heavy metals, in particular lead, can have severe and poisonous effects on human beings and marine organisms even at trace levels [3,4].

Pb(II), a soft blue-gray metallic element, has been widely used in diverse industrial areas such as paints, batteries, leaded glasses, fuels, pigments, photographic materials, petrochemicals, mining, etc. [5]. Pb(II) is considered to be a cumulative poison and found to be hazardous at high levels. Due to its toxicity, Pb(II) can cause damage to the digestive tract, immune system, human circulatory system, liver, and kidney [6].

With the rapid development of industries, discharge of wastewater containing metals ions has been on the rise,

\* Corresponding author.

which has negative impact on the surrounding ecological environments [7]. Most industrial wastewaters contain high concentrations of Pb(II), which can cause irreversible damage to human and animal health and pollute water resources [8]. Pb(II) can bioaccumulate at low concentrations in humans, causing toxic effects and even carcinogenesis [9]. Thus, its contamination has become a serious problem. Various methods, such as coagulation–flocculation, ion exchange, and electrochemical treatment, have been employed to separate lead from aqueous solutions [10,11]. However, the drawbacks of these techniques include high operating costs, difficulty in scaling up, and the generation of a large volume of toxic sludge [12,13].

As a result, adsorbent separation processes have attracted the attention of researchers because of their relatively simple operational processes, selectivity, sensitivity, low by-product formation potential, low cost, and easy regeneration procedures [14–16].

Biosorption utilizes low-cost biosorbents such as grape shoot, olive root, peat, rose wastes, bacteria, yeasts, fungi, microalgae, and marine macroalgae for the elimination of heavy metals from wastewaters [17,18]. Algal biomass has significant and various affinities towards a number of heavy metals as sorbent materials [19].

The immobilization of algal biomass is an important phase in the commercial scale-up of metal biosorption. Immobilization, unlike algal biomass in its natural state, gives biosorbent particles the density, suitable size, and mechanical strength that continuous systems need [20]. Immobilization can also save up to 50%–70% of the overall separation cost of the biomass from the processed solution. This method can also be used to regenerate biomass in several adsorption–desorption phases. Currently, alginate, chitosan, porous resin, and activated charcoal have been tested as carriers for immobilizing cells [21].

Alginate is a linear copolymer that makes up a significant percentage of the dry weight of all algae species, and each constituent residue naturally comprises carboxyl groups. The carboxylate function is supposed to be responsible for its high affinity for divalent cations like cadmium, copper, cobalt, and others [21]. The process of forming alginate beads (structure of “egg-box”) by dropping a mixture comprising biosorbents and Na-alginate into a solution of calcium chloride has been widely studied. Calcium atoms can cross-link and form salt bridges between the blocks of guluronic acid of alginate chains pair [22]. Since alginate has good biocompatibility, low cost, binding capacity, and good hydrophilicity [23], it was used in this study as a carrier for immobilization of the marine macroalgae.

According to the literature, the elimination of heavy metals by bioadsorbent [24–26] is widely studied; however, the elimination of heavy metals by immobilized algal is poorly studied.

Also, in most studies, equilibrium data using regression coefficients are used to match isotherms and kinetics. But employment of regression coefficient alone will not be enough for adaptability. Therefore, for more accuracy, different error coefficients were used in this study.

Our objective was to test the adsorption efficiency of immobilized *Gracilaria corticata* algal, which is very abundant in Iran, for the elimination of Pb(II). The optimization

of the experimental operating conditions such as the mixing time, the initial pH, the amount of Pb(II) and immobilized *Gracilaria corticata* (immobilized-GC), and the temperature was carried out. Various techniques were carried out to examine the as prepared bioadsorbents characteristics, that is, scanning electron microscopy (SEM), Brunauer–Emmett–Teller/Barrett–Joyner–Halenda (BJH), and Fourier transform infrared spectroscopy (FTIR). The kinetic, isotherm and thermodynamic models were applied to explain the adsorption behavior. Also, error functions were calculated.

## 2. Materials and methods

### 2.1. Chemicals

Pb(II) nitrate solution ( $\text{Pb}(\text{NO}_3)_2$ ) was used to synthesize the Pb(II) aqueous solution and purchased from Merck Co., Germany. Sodium alginate or Na-alginate (216.12 g/mol and  $\text{NaC}_6\text{H}_7\text{O}_6$ ) was purchased from PubChem Co., USA. Sigma Aldrich supplied NaOH and HCl. All solutions were prepared using distilled water. All chemicals were of analytical grade and used without further purification.

### 2.2. Immobilization of algal biomass

*Gracilaria corticata* algae were collected from the Chab-ahar coast in Sistan and Baluchestan province, Iran. The GC was vigorously washed with tap water for the removal of salts. The epiphytic microorganisms were then washed with distilled water, dried to a constant weight in an oven at 80°C at 120 min, ground, and sieved into 80–125  $\mu\text{m}$  fractions.

The GC biomass was immobilized by dissolving 2 g of Na-alginate in 50 mL distilled water for 30 min at 80°C with constant stirring. Based on available standards and studies, the most effective amount of biomass was 2 g [23]. After cooling, 2 g of GC biomass was added to the solution of Na-alginate and stirred for 10 min at room temperature. The mixture of Na-alginate-GC biomass was dropped into a solution of 2%  $\text{CaCl}_2$ . To enhance the mechanical strength of the beads, they were soaked in the solution of calcium chloride for 2 h at room temperature with stirring gently. For removing residual  $\text{Ca}^{2+}$  from the adsorbent surfaces, they were washed three times with distilled water and then placed in the refrigerator at 4°C before use in the experiments.

Adsorbent properties were determined using Fourier transform infrared spectroscopy (FTIR) technique (Thermo Fisher Scientific model FTIR is 10, USA), and scanning electron microscope (SEM-JEOL, JSM-IT300) methods. The Brunauer–Emmett–Teller (Micromeritics, 3Flex) method was used to determine the specific surface area and pore volume of the adsorbent.

### 2.3. Adsorption studies

Five adsorption experiment series were implemented on immobilized-GC adsorbents at different adsorption circumstances, including initial Pb(II) concentration, adsorption temperature, adsorbent dosage, and initial pH of the solution. All Pb(II) adsorption experiments were done in batch

mode scale under various experimental conditions, including concentration 10–100 mg/L, mixing time 10–120 min, immobilized-GC dosage (0.025–0.25 g per 100 mL of Pb(II) solution), pH 2–8, and temperature 20–50°C with continuous shaking. The amount of Pb(II) in the solution was measured via atomic absorption spectrometry (AAS-AGILENT 280FS AA).

Eqs. (1) and (2) were used to calculate the amount of Pb(II) uptake and Pb(II) removal % [27,29].

$$q_i = \frac{(C_0 - C_i)V}{m}; \quad i = e, t \quad (1)$$

$$\text{Pb(II) removal\%} = \frac{(C_0 - C_t)}{C_0} \times 100 \quad (2)$$

#### 2.4. Error analysis

The best isotherm and kinetic models were determined by the correlation coefficient ( $R^2$ ) analysis. Although this is useful in determining the efficiency of the correlation analysis, this analysis has limitations in solving isotherm and kinetic models that are not inherently linear. Therefore, we used three error functions to find a suitable model to represent the experimental data [30,31]. The error functions used are expressed as Eqs. (3)–(5).

$$\text{Sum of squared errors (SSE)} = \sum_{i=1}^n (q_{e,\text{cal}} - q_{e,\text{meas}})_i^2 \quad (3)$$

$$\text{Sum of absolute errors (SAE)} = \sum_{i=1}^n (q_{e,\text{cal}} - q_{e,\text{meas}})_i \quad (4)$$

$$\text{Average relative error (ARE)} = \frac{100}{n} \sum_{i=1}^n \left( \frac{q_{e,\text{cal}} - q_{e,\text{meas}}}{q_{e,\text{meas}}} \right)_i \quad (5)$$

### 3. Results and discussion

The morphology of the adsorbent was characterized by SEM (Fig. 1a and b). Fig. 4a shows that immobilized-GC has a highly rough surface with a large number of pores, indicating that there is considerable potential for biosorption of Pb(II). The decrease in the number of pores on the adsorbent surface occurred after the adsorption of Pb(II) (Fig. 4b), which indicates the adsorption of Pb(II) on the adsorbent surface. Additionally, as a result of the Pb(II) ions accumulation on the cell surface, the surface of free and immobilized-GC biomass has shrunk, become more irregular, and has spots.

The FTIR analysis for determining the functional groups was performed, and its results, before and after Pb(II) uptake, are shown in Fig. 2c and d. A strong peak at 3,422  $\text{cm}^{-1}$ , representing the stretching of the O–H and N–H bonds of the amine groups, was shifted after Pb(II) adsorption, which suggests that the bonds of O–H and N–H are involved in Pb(II) ion adsorption. The band at 2,921  $\text{cm}^{-1}$

represents C–H bonds, showing the presence of carboxylic groups from fractions of phospholipids and lipids in biomass. Peaks at 1,785 and 1,517  $\text{cm}^{-1}$ , suggesting that the C=O and S groups are involved in the biosorption of Pb(II). The absorption peaks at 1,623  $\text{cm}^{-1}$  were interrelated to the stretching vibration of C=N. The band at 1,471  $\text{cm}^{-1}$  shifted to 1425, which was related to  $\text{CH}_2$  and  $\text{CH}_3$  bending of methyl and C–O stretching vibration of carboxylic group, respectively. The peaks at 1,293  $\text{cm}^{-1}$  present after biosorption of Pb(II) ions assigned to stretching vibration of C–C–O. Also, peak at 1,162  $\text{cm}^{-1}$  represents stretching vibrations of hydrogen-bonding C–OH groups, implying the presence of carbohydrate. The band at 1,081  $\text{cm}^{-1}$  which indicates stretching vibrations of C–O (primary alcohol), was moved to 1,074  $\text{cm}^{-1}$  after Pb(II) biosorption. Furthermore, the shift of the band at 895 to 882  $\text{cm}^{-1}$  reveals Pb(II) ion binding to the amine group present on the algal surface.

In Fig. 1e, f, the  $\text{N}_2$  adsorption–desorption isotherms of immobilized-GC are depicted. According to the IUPAC system, the results were found to be type IV isotherm and exhibited an H3 hysteresis loop at  $0.5 < p/p_0 < 1.0$ . Further, the BJH average pore diameters of immobilized-GC proved to be 9.1 nm. The values of the average pore diameters determined that the adsorbent had a mesoporous structure according to IUPAC classification. In addition, the average pore volumes and average surface area of immobilized-GC were 0.12  $\text{cm}^3/\text{g}$  and 84.2  $\text{m}^2/\text{g}$ .

Table 1 shows the energy-dispersive X-ray spectroscopy results for immobilized-GC and GC adsorbents. As can be seen, Na in the synthesized adsorbent has replaced other elements, and there is about 6% Na. In general, the adsorbent is composed of the main elements of nitrogen, carbon, oxygen, and other elements are present in small amounts.

#### 3.1. Effect of effective parameters on Pb(II) uptake

The effect of the initial pH on the percentage of Pb(II) removed was investigated at pH values of 2–8 using an initial immobilized-GC mass of 0.1 g with 100 mL of contaminated solution. The initial Pb(II) concentration was 25 mg/L at 30°C  $\pm$  2°C. The mixture was shaken for 75 min at a constant stirring velocity of 120 rpm. The adsorption percentage increased as the initial pH of the solution increased from pH 2 to 6 (Fig. 2a). The surface of the immobilized-GC became more negatively charged, and subsequently, the electrostatic attraction (ion exchange) between the metal ions and the surface of the adsorbent probably increased [30]. The increase in adsorption percentage may be attributed to the interaction of  $\text{Pb}^{2+}$ ,  $\text{Pb}(\text{OH})^+$ , and  $\text{Pb}(\text{OH})_2$  with the functional groups present on the surface of the adsorbents due to ion exchange mechanism or by hydrogen bonding [31].

Also, the value of  $\text{pH}_{\text{PZC}}$  for adsorbent is 6.5, Fig. 2a. At pH below  $\text{pH}_{\text{PZC}}$ , the adsorbent surface has a higher negative charge which allows for more adsorption of Pb(II) cations. For next experiments, an optimal pH value of 6 is used. For pH values below the optimal value, competition between Pb(II) ions and  $\text{H}_3\text{O}^+$  reduces the adsorption efficiency, whereas higher pH values result in hydrolysis of Pb(II) species which encourages precipitation and prevents quantitative adsorption [32].

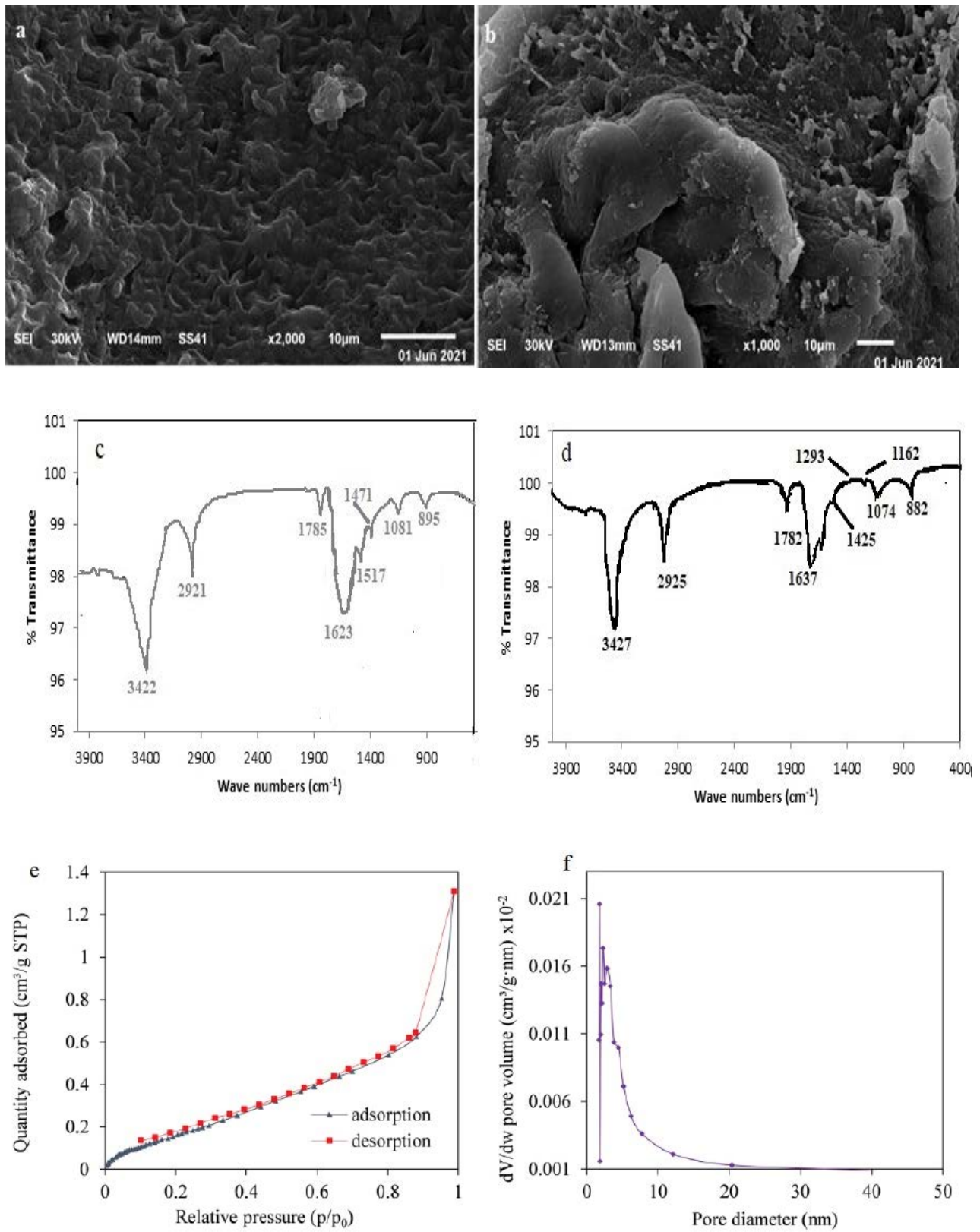


Fig. 1. SEM images of immobilized-GC before (a) and after of adsorption (b) FTIR spectra before (c) and after of adsorption (d) N<sub>2</sub> adsorption-desorption isotherms (e) pore-size distributions from the adsorption branches through the BJH method (f).

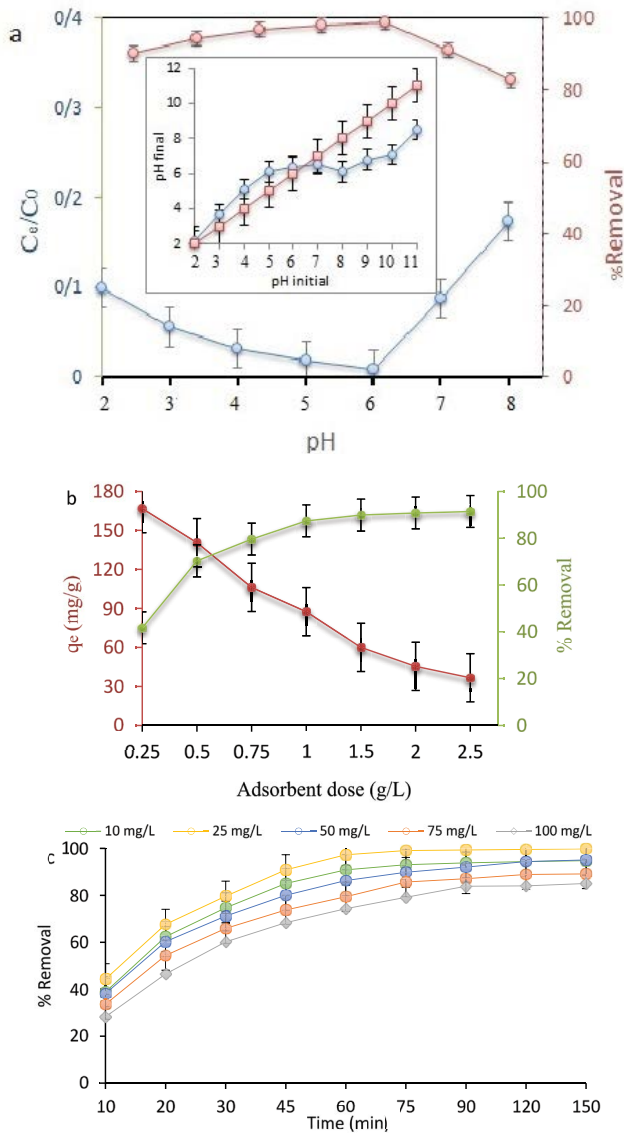


Fig. 2. Effect of pH inset: determine the  $pH_{ZPC}$  (a), effect of adsorbent dose on Pb(II) removal (b), effect of contact time and concentration (c), and effect of temperature on Pb(II) removal (d).

This experiments was conducted with different concentrations of adsorbents (i.e., 0.25, 0.5, 0.75, 1, 1.5, 2, and 2.5 g/L) at the optimal initial pH value, with 100 mL of the pollutant solution. The Pb(II) amount was 100 mg/L at  $30^{\circ}\text{C} \pm 2^{\circ}\text{C}$ , and the mixture was shaken for 90 min at a constant stirring velocity of 120 rpm. The maximum removal efficiency was obtained to be 99.1%, at a corresponding immobilized-GC dosage of 1 g/L as shown in 2b. The adsorption percentage increases as the doses of the immobilized-GC in the solution increase from 0.25 to 1 g. These results can be due to the fact that increasing the adsorbent dose from 0.25 to 1 g provides more active binding sites for the adsorption process [33]. Thus, more Pb(II) ions are adsorbed onto the surface of the adsorbent since the competition between molecules for active binding sites

Table 1

Important properties of the LMAC GC and immobilized-GC

Element	GC		Immobilized-GC	
	% weight	% Atomic	% weight	% Atomic
N	11.3	12.1	11.2	11.5
O	38.4	38.1	34.85	34.5
C	47.2	46.9	44.2	45.1
Others	3.1	2.9	3.85	4.74
(Si, K, Cl, Ca				
Na	–	–	5.9	6.1

is reduced [34]. The optimal dose obtained was 1 g, which was applied for the subsequent batches.

This batch of experiments was conducted at different contact times (10, 20, 30, 45, 60, 75, 90 and 120 min) at optimal pH value and adsorbent dose at room temperature of  $30^{\circ}\text{C} \pm 2^{\circ}\text{C}$  using 100 mL of pollutant solution. The Pb(II) amount was 25 mg/L at a constant stirring velocity of 120 rpm. The maximum removal efficiencies obtained were 99.1% at a contact time of 75 min as illustrated in Fig. 2c. The adsorption percentage increases with increasing contact time from 10 to 75 min. However, it appears that the rate of Pb(II) uptake is the greatest within the initial 30 min because of the availability of active binding sites on the surface of the immobilized-GC [35]. Consequently, it can be seen that the equilibrium of Pb(II) uptake by the adsorbent is reached within 75 min, and after that, there was an insignificant change in Pb(II) uptake until 120 min. The study of Pb(II) adsorption was also performed using GC biomass and alginate; it was observed that for a concentration of 25 mg/L, the removal efficiencies using mentioned adsorbents were 89.1% and 78.2% after 120 min, respectively.

This batch was conducted at different concentrations of Pb(II) including 10, 25, 50, 75, and 100 mg/L at the optimal pH value and the optimal immobilized-GC dose obtained from previous batches using 100 mL of contaminated solution at  $30^{\circ}\text{C} \pm 2^{\circ}\text{C}$ . The mixture was shaken for 75 min at a constant stirring velocity of 150 rpm. The maximum removal efficiencies were 99.1% at Pb(II) amount of 25 mg/L, as shown in Fig. 2c. The results suggest that the percentage of Pb(II) removal by adsorption increases as the Pb(II) amount increases to a certain extent. The adsorption percentage increased from 93.2% to 99.1% as the Pb(II) amount was increased from 10 to 25 mg/L. Thereafter, the percentage of Pb(II) removal decreases as the Pb(II) amount increases to a value of 100 mg/L. This can be interpreted as at a fixed amount of adsorbent, the high initial Pb(II) concentration leads to an excess amount of available particles compared with the active binding site on the adsorbent surface, so that, the percentage of Pb(II) removal by adsorption decreases [36].

This batch was conducted at different temperature values (e.g., 293, 303, 313 and 323 K ( $20^{\circ}\text{C}$ – $50^{\circ}\text{C}$ )) at an optimal pH of 6.0, an optimal dose of adsorbents equal to 0.1 g, and 100 mL contaminated solution of 100 mg/L Pb(II). The mixture was shaken for 75 min at a constant stirring velocity of 120 rpm. The maximum removal efficiencies were

99.4% at a temperature of 323 K°C as shown in Fig. 2d; this indicates that the adsorption process is an endothermic reaction [37].

### 3.2. Isotherm study

The isotherm study was conducted by varying the amount of Pb(II) in synthetic wastewater from 10 to 100 mg/L. The experiment was performed by adding immobilized-GC into 100 mL flasks containing Pb(II) solution. Then, the contents were mechanically stirred at 120 rpm for a given time at different temperatures. Next, the solutions were filtered using Whatman filter paper having an average pore size of 0.45  $\mu\text{m}$ . The data obtained from the experiment were linearly fitted for the different isotherms as described as follows.

### 3.3. Langmuir isotherm

The Langmuir isotherm quantitatively describes the monolayer adsorption on the outer surface of the immobilized-GC. The Langmuir isotherm can be expressed as follows [38,39]:

$$\frac{1}{q_e} = \frac{1}{q_m} + \frac{1}{K_L C_e q_m} \quad (6)$$

### 3.4. Freundlich isotherm

The Freundlich isotherm is an empirical adsorption model, which can be applied to nonideal biosorption on heterogeneous surfaces as well as multilayer sorption. The isotherm is displayed as shown in Eq. (7) [40,41]:

$$\log q_e = \frac{1}{n} \log C_e + \log K_F \quad (7)$$

### 3.5. Temkin isotherm

The Temkin isotherm contains a factor that explicitly takes into account adsorbent–adsorbate interactions. As implied in the equation, its derivation is characterized by a uniform distribution of binding energies and is expressed as in Eq. (8) [42].

$$q_e = B \ln K_T + B \ln C_e \quad (8)$$

### 3.6. Dubinin–Radushkevich isotherm

The last isotherm is the Dubinin–Radushkevich model, which describes the adsorption energy between adsorbate and adsorbent in terms of the adsorption potential ( $\epsilon$ ). The Dubinin–Radushkevich isotherm model can be described by Eqs. (9)–(11) [44,45]:

$$\log q_e = \ln q_m - \beta \epsilon^2 \quad (9)$$

$$\epsilon = RT \ln \left[ 1 + \frac{1}{C_e} \right] \quad (10)$$

$$E = \left[ \frac{1}{\sqrt{2\beta}} \right] \quad (11)$$

The value of  $\beta$  can be calculated from the slope by plotting the straight line between  $\ln q_e$  and  $\epsilon^2$ .

The fit of the model with the experimental results was evaluated using linear regression analysis, as seen in Table 2. Thus, it is noted that the  $R^2$  obtained at all temperatures from the Langmuir isotherm was the highest. Such a high value indicated that the Langmuir isotherm was the best model for Pb(II) adsorption, suggesting monolayer adsorption on the heterogeneous surface. Similar results were reported when adsorbents from polypyrrole composites were used to remove Pb(II) ions [46]. The maximum adsorption capacity,  $q_{\text{max}}$ , was 89.1, 98.3, 108.2, and 122.1 mg/g at 20°C, 30°C, 40°C, and 50°C, respectively. According to the obtained values of the separation factor or equilibrium

Table 2  
Isotherm parameters for adsorption of Pb(II) at various temperatures

Isotherm models	293 K	303 K	313 K	323 K
Langmuir				
$q_m$ (mg/g)	89.1	98.3	108.2	122.1
$K_L$ (L/mg)	0.0041	0.0056	0.0081	0.0095
$R_L$	0.711	0.641	0.552	0.512
$R^2$	0.996	0.997	0.999	0.995
SSE	1.45	1.29	2.35	2.17
SAE	1.76	2.13	1.32	1.24
ARE	2.17	1.79	1.46	1.19
Freundlich				
$K_F$	8.17	11.2	13.4	15.8
$1/n$	0.276	0.176	0.347	0.463
$R^2$	0.871	0.895	0.902	0.923
SSE	6.14	4.84	5.38	8.21
SAE	7.35	6.56	3.87	5.05
ARE	5.72	9.52	7.05	7.09
Temkin				
$K_T$	3.17	5.27	6.34	7.93
$B$	51.2	58.3	71.2	79.5
$R^2$	0.812	0.798	0.752	0.832
SSE	7.25	11.9	7.14	9.27
SAE	9.12	7.43	9.25	12.3
ARE	11.8	9.27	8.43	8.29
Dubinin–Radushkevich				
$q_m$ (mg/g)	87.2	92.3	99.2	107.1
$E$	7.96	8.45	9.23	10.27
$R^2$	0.911	0.932	0.971	0.906
SSE	11.2	6.25	11.7	9.84
SAE	7.42	7.41	8.24	7.48
ARE	7.13	9.17	9.16	6.29

constant,  $R_L$  was between 0.15 and 0.37, which indicated the favorability of the adsorption process.

The  $(1/n)$  value is less than unity. It means that the adsorption process is preferred, the surface is heterogeneous, and there are fewer interactions between the adsorbed ions. It also means that Pb(II) adsorption occurs through multi-molecular and multi-anchorage adsorption mechanisms.

The higher Elovich parameters ( $\beta$  and  $\alpha$ ), determined from the slope and intercept of the plotting of  $q_t$  against  $\ln t$ , respectively, indicate a greater rate of chemical sorption confirming the adsorption type of pseudo-second-order.

The mean biosorption energy ( $E$ , kJ/mol) reveals the physical or chemical biosorption process. Since the  $E$  value was greater than 8 kJ/mol (Table 1), it was hypothesized that Pb(II) biosorption was accomplished by a chemisorption process [46,47].

Several adsorbents from other studies were compared with the adsorbents used in this research in terms of their adsorption capacities, and the comparison is presented in Table 3. According to this comparison, immobilized-GC has a promising future as an adsorbent in wastewater treatment, as approved by their excellent results.

### 3.7. Kinetics study

In order to clarify the reaction order and rate-controlling mechanism, the following linear kinetic models were employed.

The pseudo-first-order kinetic model assumes that the number of sites that solutes can occupy is proportional to the rate of adsorption. The model is written as in Eq. (12) [49]:

$$\log(q_e - q_t) = \log q_e - \frac{K_1}{2.303} t \quad (12)$$

Table 3  
Comparison of the adsorption capacities of Pb(II) using various adsorbents

Material	Adsorption capacity ( $q_{\max}$ ) mg/g	Reference
Metal-organic framework MIL-100(Fe)	22.8	[44]
PDA@rGO/Fe <sub>3</sub> O <sub>4</sub>	35.2	[45]
AC-Sea buckthorn stones	45.2	[8]
<i>Lemna minor</i>	32.2	[10]
Polypyrrole	35.6	[13]
Bael leaves	54.2	[19]
AC- <i>Juniperus procera</i> leaves	26.1	[25]
Chitosan	48.3	[31]
Carbon aerogel	0.75	[46]
Zeolite/CuO NCs	41.2	[47]
Modified palygorskite clay	27.6	[48]
Immobilized-GC	293 K = 89.1 303 K = 98.3 313 K = 108.2 323 K = 122.1	This research

The pseudo-second-order kinetic model involves chemisorption, where the removal of adsorbate from the bulk liquid is due to the physiochemical interaction between adsorbent and adsorbate. The pseudo-second-order kinetic model is shown in Eq. (13) [50]:

$$\frac{t}{q_t} = \frac{1}{K_2 q_e^2} + \frac{t}{q_e} \quad (13)$$

As for the intraparticle diffusion model, it is noted that intraparticle diffusion transport is the slowest step of the adsorption process between adsorbate and adsorbent as compared to film diffusion and pore diffusion. The intraparticle diffusion model can be written as in Eq. (14) [51]:

$$q_t = K_b t^{1/2} + C \quad (14)$$

In Table 4 and Fig. 3a and b, linear regression analysis and kinetic parameters of pseudo-second-order, pseudo-first-order, and intraparticle diffusion models were given. Results revealed that the pseudo-second-order model yielded a higher correlation coefficient ( $R^2 = 0.99$ ) for different concentrations compared to the pseudo-first-order and the intraparticle diffusion models. This observation indicated that the pseudo-second-order was the most suitable model for Pb(II) adsorption using immobilized-GC. Furthermore, previous researchers have reported pseudo-second-order as the best fit model for metal adsorption when using adsorbents prepared from graphene oxide-Fe<sub>3</sub>O<sub>4</sub>@polydopamine [52]. Moreover, the magnitude of the adsorption capacity of the pseudo-second-order model ( $q_e$  cal) was found to be comparable to the value obtained experimentally ( $q_e$  exp). Such a result confirmed the validity of the pseudo-second-order, proving that the kinetic model applied for Pb(II) adsorption using immobilized-GC was the most suitable. The error coefficient for the pseudo-second-order kinetics is less than the pseudo-first-order kinetics. The intraparticle diffusion model describes the basic diffusion processes that occur. Fig. 3b shows the data of linear regression of  $q_t$  against  $t^{0.5}$  plots, indicating multilinearity (three phases). The slope of the plotting  $q_t$  against  $t^{0.5}$  was used to calculate the rate constant of intraparticle diffusion ( $K_b$ ) as seen in Table 4. The  $q_t$  against  $t^{0.5}$  plots in any of the cases did not pass through the origin ( $C_i > 0$ ), implying that intraparticle diffusion was not the only rate-limiting stage, and external mass transfer also played a main role in the adsorption of Pb(II) by immobilized-GC [53].

### 3.8. Thermodynamic study

The thermodynamic study of the Pb(II) adsorption process was carried out at 293, 303, 313, and 323 K; the initial concentration of Pb(II) in the solution, pH of the solution, the dosage of adsorbent, and contact time were maintained according to the optimal conditions. The change in the standard  $\Delta G^\circ$  for the adsorption process can be calculated, as in Eq. (15) [54].

$$\Delta G^\circ = -RT \ln K_L \quad (15)$$

Table 4  
Results of kinetic model related to the Pb(II) adsorption onto immobilized-GC

Model	Parameters	10 mg/L	25 mg/L	50 mg/L	75 mg/L	100 mg/L
Pseudo-first-order	$q_e$ exp	9.48	24.9	47.5	66.9	85.1
	$q_e$ cal	4.32	12.4	23.6	32.9	51.1
	$K_1$	0.031	0.051	0.058	0.056	0.064
	$R^2$	0.843	0.892	0.902	0.883	0.905
	SSE	9.11	9.32	11.6	10.2	9.25
	SAE	7.24	10.2	9.24	14.3	10.7
	ARE	11.6	9.25	7.27	7.56	8.23
Pseudo-second-order	$q_e$ cal	9.81	27.2	49.4	71.3	89.2
	$K_2$	0.0071	0.0053	0.0041	0.0029	0.0017
	$R^2$	0.997	0.994	0.997	0.997	0.995
	SSE	1.41	1.61	1.27	1.43	1.87
	SAE	1.39	1.41	1.65	1.91	2.16
	ARE	1.53	1.12	1.08	1.44	1.08
	Stage 1					
Intraparticle diffusion	$K_b$	6.19	7.11	9.85	13.1	16.5
	$C$	2.25	3.97	5.76	8.45	10.4
	$R^2$	0.931	0.912	0.845	0.871	0.904
	Stage 2					
	$K_b$	1.85	2.45	4.11	6.24	7.21
	$C$	3.97	6.14	13.3	19.2	27.6
	$R^2$	0.924	0.911	0.917	0.895	0.902
	Stage 3					
	$K_b$	0.532	0.681	0.765	0.795	0.873
	$C$	5.65	9.44	17.4	26.4	31.3
$R^2$	0.889	0.914	0.932	0.874	0.893	

The change in the  $\Delta G^\circ$  is related to the  $\Delta H^\circ$  and  $\Delta S^\circ$  via the Gibbs–Helmholtz equation ( $\Delta G^\circ = \Delta H^\circ - T\Delta S^\circ$ ). Thus,  $k_c$  becomes [55]:

$$\ln K_L = \frac{\Delta S^\circ}{R} - \frac{\Delta H^\circ}{RT} \quad (16)$$

Eq. (13) is the Van't Hoff equation in linear form. Thus, plotting  $\ln K_L$  vs.  $1/T$  yielded a straight line, whose slope and  $y$ -intercept yielded  $\Delta S^\circ$  and  $\Delta H^\circ$ , respectively.

Table 5 shows the results of thermodynamic parameters. A positive value was observed for  $\Delta H^\circ$ , which designates that the process of adsorption was endothermic. Previous research also reported the same outcome of the endothermic Pb(II) adsorption process when employing carbon prepared from *Enteromorpha prolifera* [41]. The positive value of  $\Delta S^\circ$  indicated an increase in randomness at the adsorbent solution interface [56]. However, negative values of  $\Delta G^\circ$  demonstrated that the adsorption process was both thermodynamic and spontaneous, which is quite feasible; the increase of  $\Delta G^\circ$  with temperature implies that the process favors higher energy input [57].

### 3.9. Adsorbent regeneration

Adsorbent recovery was performed in 5 steps. After the adsorption process, the adsorbent was collected using

Table 5  
Values of thermodynamic parameters for the adsorption of Pb(II) onto immobilized-GC

Temperature (K)	$\Delta G^\circ$ (kJ/mol)	$\Delta H^\circ$ (kJ/mol)	$\Delta S^\circ$ (kJ/mol K)
293	-2.58		
303	-4.15	52.01	0.185
313	-5.49		
323	-8.37		

a 0.2-micron filter, washed twice with distilled water, and finally dried at 80°C. The experiment was performed under optimal conditions obtained from the previous steps ( $C_0$ : 25 mg/L, initial pH: 6.0, contact time: 90 min, adsorbent dose: 2 g/L, and  $T$ : 298 K). The results were shown in Fig. 4, and as can be seen, after five steps, the removal percentage decreases by about 12%. It can be due to the loss of adsorbent during washing and collection [58,59].

## 4. Conclusion

This study investigates the sorption of Pb(II) onto the immobilized-GC surface under different reaction conditions such as contact time, pH, Pb(II) ion concentration, and temperature in a batch study. From the results obtained,

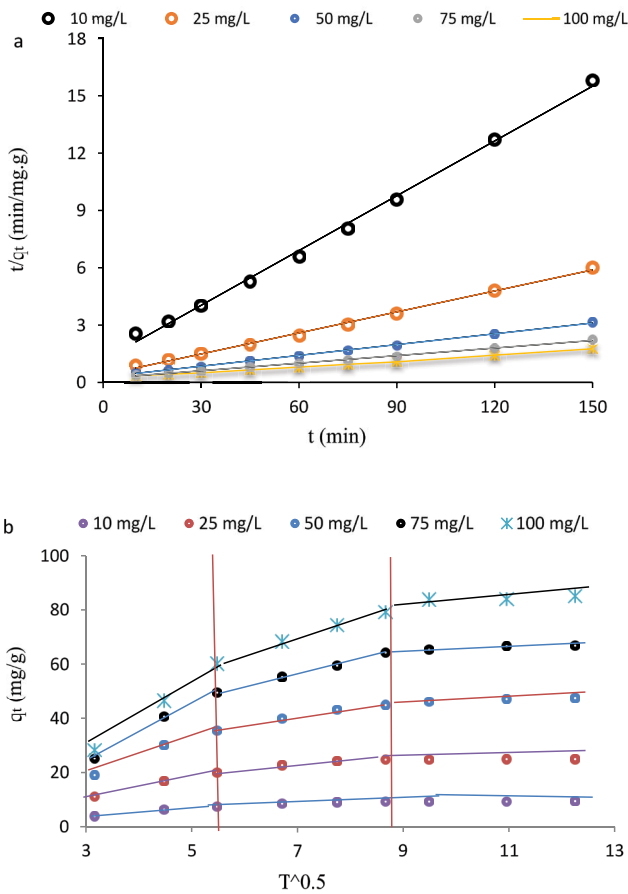


Fig. 3. Pseudo-second-order (a), intraparticle diffusion (b), plots for the kinetic modeling of Pb(II) adsorption onto immobilized-GC at different concentrations.

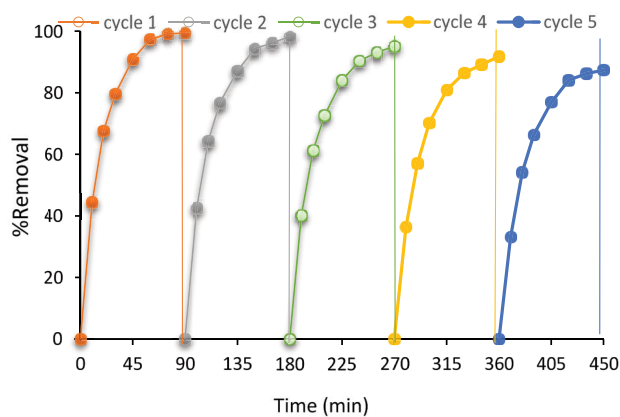


Fig. 4. Recyclability properties of immobilized-GC for Pb(II) adsorption.

it can be concluded that pH is one of the key factors affecting the rate of sorption. After applying the optimal values of the studied adsorption parameters, the adsorption kinetics were investigated using different models, such

as pseudo-first-order, pseudo-second-order, and intraparticle diffusion equation, and pseudo-second-order best fits the adsorption of Pb(II). The intraparticle diffusion adsorption model showed that the adsorption was a multistep controlled mechanism. The optimum conditions were achieved at pH of 6, initial Pb(II) concentration of 10 mg/L at 75 min with an adsorption capacity of 24.9 mg/g at room temperature. Due to the high regression coefficient and the lower error coefficient at all temperatures, the Langmuir isotherm model best described the adsorption. According to thermodynamic studies, the negative and positive values were obtained for  $\Delta G^\circ$  and  $\Delta H^\circ$ ; these values are representative of the spontaneous and feasible nature and endothermic nature of sorption, respectively. In the end, it can be concluded that under the optimal conditions adopted in this study, Pb(II) removal from aqueous solutions by adsorption is best obtained using immobilized-GC.

**Symbols**

$C_0$	—	Concentrations of Pb(II) in mg/L at the start
$C_t$	—	Concentrations of Pb(II) in mg/L after time $t$
$C_e$	—	Concentrations of Pb(II) in mg/L at equilibrium
$V$	—	Pb(II) volume at mL
$m$	—	Immobilized-GC masses in mg
$K_L$	—	Langmuir adsorption constant, L/mg
$K_F$	—	Freundlich constant, L/g
$n$	—	Heterogeneity factor. If the value of $n < 1$ , the adsorption is a chemical process; if $n > 1$ , then it is a physical process.
$q_e$	—	Adsorption capacity at equilibrium
$q_m$	—	Maximum adsorption capacity
$R_L$	—	Dimensionless separation factor. The values of $R_L$ show whether the biosorption process is irreversible ( $R_L = 0$ ), linear ( $R_L = 1$ ), favorable ( $0 < R_L < 1$ ) or undesirable ( $R_L > 1$ )
$\Delta G^\circ$	—	Gibbs free energy, kJ/mol
$\Delta S^\circ$	—	Entropy, kJ/mol
$\Delta H^\circ$	—	Enthalpy, kJ/mol
$K_1$	—	Equilibrium rate constant for pseudo-first-order kinetics, 1/min
$K_2$	—	Equilibrium rate constant for pseudo-second-order kinetics, g/mg min
$K_b$	—	Intraparticle diffusion rate constant, mg/g min <sup>1/2</sup>
$C$	—	Thickness of the boundary layer
$\beta$	—	Dubinin–Radushkevich isotherm constant, mol <sup>2</sup> /kJ <sup>2</sup>
$\varepsilon$	—	Polanyi potential
$E$	—	Adsorption energy, kJ/mol
$K_T$	—	Constant of equilibrium binding, L/mg
$B$	—	Temkin constant associated with the heat of adsorption, J/mol
$pH_{PZC}$	—	Point of zero charge
D-R	—	Dubinin–Radushkevich

## Acknowledgement

We are grateful to the student research committee of Zahedan University of medical sciences for their financial code: 10759.

## References

- [1] D. Balarak, H. Azarpira, F.K. Mostafapour, Thermodynamics of removal of cadmium by adsorption on Barley husk biomass, *Pharm. Chem.*, 8 (2016) 243–247.
- [2] H. Azarpira, Y. Mahdavi, D. Balarak, Removal of Cd(II) by adsorption on agricultural waste biomass, *Pharm. Chem.*, 8 (2016) 61–67.
- [3] Md. Rabiul Awual, Md. Munjur Hasan, A ligand based innovative composite material for selective lead(II) capturing from wastewater, *J. Mol. Liq.*, 294 (2019) 111679, doi: 10.1016/j.molliq.2019.111679.
- [4] M.S. Al-Harashsheh, K. Al Zboon, L. Al-Makhadmeh, M. Hararah, M. Mahasneh, Fly ash based geopolymer for heavy metal removal: a case study on copper removal, *J. Environ. Chem. Eng.*, 3 (2015) 1669–1677.
- [5] M. Attari, S.S. Bukhari, H. Kazemian, S. Rohani, A low-cost adsorbent from coal fly ash for mercury removal from industrial wastewater, *J. Environ. Chem. Eng.*, 5 (2017) 391–399.
- [6] K.D. Ogundipe, A. Babarinde, Comparative study on batch equilibrium biosorption of Cd(II), Pb(II) and Zn(II) using plantain (*Musa paradisiaca*) flower: kinetics, isotherm and thermodynamics, *Chem. Int.*, 2 (2017) 135–149.
- [7] S. Hosseini, H.N.M. Ekramul Mahmud, R. Yahya, Polymer adsorbent for the removal of lead ions from aqueous solution, *Int. J. Tech. Res. Appl.*, 11 (2014) 4–8.
- [8] S.Z. Mohammadi, M.A. Karimi, D. Afzali, F. Mansouri, Removal of Pb(II) from aqueous solutions using activated carbon from Sea-buckthorn stones by chemical activation, *Desalination*, 262 (2010) 86–93.
- [9] Md. Rabiul Awual, Innovative composite material for efficient and highly selective Pb(II) ion capturing from wastewater, *J. Mol. Liq.*, 284 (2019) 502–510.
- [10] N.H. Yarkandi, Removal of lead(II) from waste water by adsorption, *Int. J. Curr. Microbiol. Appl. Sci.*, 3 (2014) 207–228.
- [11] Md. Rabiul Awual, An efficient composite material for selective lead(II) monitoring and removal from wastewater, *J. Environ. Chem. Eng.*, 7 (2019) 103087, doi: 10.1016/j.jece.2019.103087.
- [12] Md. Rabiul Awual, Mesoporous composite material for efficient lead(II) detection and removal from aqueous media, *J. Environ. Chem. Eng.*, 7 (2019) 103124, doi: 10.1016/j.jece.2019.103124.
- [13] H.N. Muhammad Ekramul Mahmud, A. K. Obidul Huq, R.b. Yahya, The removal of heavy metal ions from wastewater/ aqueous solution using polypyrrole-based adsorbents: a review, *RSC Adv.*, 6 (2016) 14778–14791.
- [14] A. Shahat, H.M.A. Hassan, H.M.E. Azzazy, E.A. El-Sharkawy, H.M. Abdou, Md. Rabiul Awual, Novel hierarchical composite adsorbent for selective lead(II) ions capturing from wastewater samples, *Chem. Eng. J.*, 332 (2018) 377–386.
- [15] Md. Rabiul Awual, A novel facial composite adsorbent for enhanced copper(II) detection and removal from wastewater, *Chem. Eng. J.*, 266 (2015) 368–375.
- [16] Md. Rabiul Awual, Assessing of lead(III) capturing from contaminated wastewater using ligand doped conjugate adsorbent, *Chem. Eng. J.*, 289 (2016) 65–73.
- [17] T. Chen, J. Zhang, H. Ge, M. Li, Y. Li, B. Liu, T. Duan, R. He, W. Zhu, Efficient extraction of uranium in organics-containing wastewater over  $g\text{-C}_3\text{N}_4/\text{GO}$  hybrid nanosheets with type-II band structure, *J. Hazard. Mater.*, 384 (2020) 121383, doi: 10.1016/j.jhazmat.2019.121383.
- [18] D. Balarak, A. Joghataei, H. Azarpira, F.K. Mostafapour, Isotherms and thermodynamics of Cd(II) ion removal by adsorption onto *Azolla filiculoides*, *Int. J. Pharm. Technol.*, 8 (2016) 15780–15788.
- [19] E. Bazrafshan, M. Sobhanikia, F.K. Mostafapour, H. Kamani, D. Balarak, Chromium biosorption from aqueous environments by mucilaginous seeds of *Cydonia oblonga*: thermodynamic, equilibrium and kinetic studies, *Global NEST J.*, 19 (2017) 269–277.
- [20] S. Chakravarty, A. Mohanty, T. Nag Sudha, A.K. Upadhyay, J. Konar, J.K. Sircar, A. Madhukar, K.K. Gupta, Removal of Pb(II) ions from aqueous solution by adsorption using bael leaves (*Aegle marmelos*), *J. Hazard. Mater.*, 173 (2010) 502–509.
- [21] M.M. Lakouraj, F. Mojerlou, E.N. Zare, Nanogel and superparamagnetic nanocomposite based on sodium alginate for sorption of heavy metal ions, *Carbohydr. Polym.*, 106 (2014) 34–41.
- [22] Y. Liu, L. Gan, Z. Chen, M. Megharaj, R. Naidu, Removal of nitrate using *Paracoccus* sp. YF1 immobilized on bamboo carbon, *J. Hazard. Mater.*, 229 (2012) 419–425.
- [23] S.F. Mohamed, F. Agili, M.M. Asker, K. El Shebawy, Characterization of the biosorption of lead with calcium alginate xerogels and immobilized *Turbinaria decurrens*, *Monatsh. Chem.*, 142 (2011) 225–232.
- [24] Md. Rabiul Awual, Novel conjugated hybrid material for efficient lead(II) capturing from contaminated wastewater, *Mater. Sci. Eng., C*, 101 (2019) 686–695.
- [25] A.H. Mahvi, D. Balarak, E. Bazrafshan, Remarkable reusability of magnetic  $\text{Fe}_3\text{O}_4$ -graphene oxide composite: a highly effective adsorbent for Cr(VI) ions, *Int. J. Environ. Anal. Chem.*, (2021) 1910250, doi: 10.1080/03067319.2021.1910250.
- [26] I.H. Ali, M.K. Al Mesfer, M.I. Khan, M. Danish, M.M. Alghamdi, Exploring adsorption process of lead(II) and chromium(VI) ions from aqueous solutions on acid activated carbon prepared from *Juniperus procera* leaves, *Processes*, 7 (2019) 217, doi: 10.3390/pr7040217.
- [27] D.P. Facchi, A.L. Cazetta, E.A. Canesin, V.C. Almeida, E.G. Bonafé, M.J. Kipper, A.F. Martins, New magnetic chitosan/alginate/ $\text{Fe}_3\text{O}_4/\text{SiO}_2$  hydrogel composites applied for removal of Pb(II) ions from aqueous systems, *Chem. Eng. J.*, 337 (2018) 595–608.
- [28] R.-A. Dyanati-Tilaki, Z. Yousefi, J. Yazdani-Cherati, D. Balarak, The ability of *Azolla* and *Lemna minor* biomass for adsorption of phenol from aqueous solutions, *J. Mazandaran Univ. Med. Sci.*, 23 (2013) 140–146.
- [29] S. Agarwal, I. Tyagi, V.K. Gupta, M.H. Dehghani, J. Jaafari, D. Balarak, M. Asif, Rapid removal of noxious nickel(II) using novel  $\gamma$ -alumina nanoparticles and multiwalled carbon nanotubes: kinetic and isotherm studies, *J. Mol. Liq.*, 224 (2016) 618–623.
- [30] R. Dyanati, Z. Yousefi, J. Yazdani Cherati, D. Balarak, Investigating phenol absorption from aqueous solution by dried *Azolla*, *J. Mazandaran Univ. Med. Sci.*, 22 (2013) 13–20.
- [31] Y. Huang, C. Hu, Y. An, Z. Xiong, X. Hu, G. Zhang, H. Zheng, Magnetic phosphorylated chitosan composite as a novel adsorbent for highly effective and selective capture of lead from aqueous solution, *J. Hazard. Mater.*, 405 (2020) 124195, doi: 10.1016/j.jhazmat.2020.124195.
- [32] Md. Rabiul Awual, Md. Munjur Hasan, A novel fine-tuning mesoporous adsorbent for simultaneous lead(II) detection and removal from wastewater, *Sens. Actuators, B*, 202 (2014) 395–403.
- [33] Md. Rabiul Awual, Md. Munjur Hasan, A. Shahat, Functionalized novel mesoporous adsorbent for selective lead(II) ions monitoring and removal from wastewater, *Sens. Actuators, B*, 203 (2014) 854–863.
- [34] T. Depci, A.R. Kul, Y. Önal, Competitive adsorption of lead and zinc from aqueous solution on activated carbon prepared from Van apple pulp: study in single- and multi-solute systems, *Chem. Eng. J.*, 200–202 (2012) 224–236.
- [35] L. Mouni, D. Merabet, A. Bouzaza, L. Belkhir, Adsorption of Pb(II) from aqueous solutions using activated carbon developed from Apricot stone, *Desalination*, 276 (2011) 148–153.
- [36] Md. Rabiul Awual, Md. Munjur Hasan, Novel conjugate adsorbent for visual detection and removal of toxic lead(II) ions from water, *Microporous Mesoporous Mater.*, 196 (2014) 261–269.
- [37] O.E. Abdel Salam, N.A. Reiad, M.M. ElShafei, A study of the removal characteristics of heavy metals from wastewater by low-cost adsorbents, *J. Adv. Res.*, 2 (2011) 297–303.

- [38] Y. Huang, S. Li, J. Chen, X. Zhang, Y. Chen, Adsorption of Pb(II) on mesoporous activated carbons fabricated from water hyacinth using  $H_2PO_4$  activation: adsorption capacity, kinetic and isotherm studies, *Appl. Surf. Sci.*, 293 (2014) 160–168.
- [39] L. Wang, J. Zhang, R. Zhao, Y. Li, C. Li, C. Zhang, Adsorption of Pb(II) on activated carbon prepared from *Polygonum orientale* Linn.: kinetics, isotherms, pH, and ionic strength studies, *Bioresour. Technol.*, 101 (2010) 5808–5814.
- [40] W.N. Nyairo, Y.R. Eker, C. Kowenje, I. Akin, H. Bingol, A. Tor, D.M. Onger, Efficient adsorption of lead(II) and copper(II) from aqueous phase using oxidized multiwalled carbon nanotubes/polypyrrole composite, *Sep. Sci. Technol.*, 53 (2018) 1498–1510.
- [41] Y. Li, Q. Du, X. Wang, P. Zhang, D. Wang, Z. Wang, Y. Xia, Removal of lead from aqueous solution by activated carbon prepared from *Enteromorpha prolifera* by zinc chloride activation, *J. Hazard. Mater.*, 183 (2010) 583–589.
- [42] E.A. Deliyanni, G.Z. Kyzas, K.S. Triantafyllidis, K.A. Matis, Activated carbons for the removal of heavy metal ions: a systematic review of recent literature focused on lead and arsenic ions, *Open Chem.*, 13 (2015) 699–708.
- [43] Y. Zhang, Q. Xue, F. Li, J. Dai, Removal of heavy metal ions from wastewater by capacitive deionization using polypyrrole/chitosan composite electrode, *Adsorpt. Sci. Technol.*, 37 (2019), doi: 10.1177/0263617418822225.
- [44] B. Alawa, J.K. Srivastava, A. Srivastava, J. Palsania, Adsorption of heavy metal Pb(II) from synthetic waste water by polypyrrole composites, *Int. J. Chem. Stud.*, 3 (2015) 3–8.
- [45] M. Forghani, A. Azizi, M.J. Livani, L.A. Kafshgari, Adsorption of lead(II) and chromium(VI) from aqueous environment onto metal-organic framework MIL-100(Fe): synthesis, kinetics, equilibrium and thermodynamics, *J. Solid State Chem.*, 291 (2020) 121636, doi: 10.1016/j.jssc.2020.121636.
- [46] A. Mehdinia, S. Heydari, A. Jabbari, Synthesis and characterization of reduced graphene oxide- $Fe_3O_4$ @polydopamine and application for adsorption of lead ions: isotherm and kinetic studies, *Mater. Chem. Phys.*, 239 (2020) 121964, doi: 10.1016/j.matchemphys.2019.121964.
- [47] A.K. Meena, G.K. Mishra, P.K. Rai, C. Rajagopal, P.N. Nagar, Removal of heavy metal ions from aqueous solutions using carbon aerogel as an adsorbent, *J. Hazard. Mater.*, 122 (2005) 161–170.
- [48] A.A. Alswat, M.B. Ahmad, T.A. Saleh, Zeolite modified with copper oxide and iron oxide for lead and arsenic adsorption from aqueous solutions, *J. Water Supply Res. Technol. AQUA*, 65 (2016) 465–479.
- [49] L. Lv, N. Chen, C. Feng, Y. Gao, M. Li, Xanthate-modified magnetic chitosan/poly(vinyl alcohol) adsorbent: preparation, characterization, and performance of Pb(II) removal from aqueous solution, *J. Taiwan Inst. Chem. Eng.*, 78 (2017) 485–492.
- [50] D. Balarak, M. Baniyasi, S.-M. Lee, M.J. Shim, Ciprofloxacin adsorption onto *Azolla filiculoides* activated carbon from aqueous solutions, *Desal. Water Treat.*, 218 (2021) 444–453.
- [51] T.J. Al-Musawi, A.H. Mahvi, A.D. Khatibi, D. Balarak, Effective adsorption of ciprofloxacin antibiotic using powdered activated carbon magnetized by iron(III) oxide magnetic nanoparticles, *J. Porous Mater.*, 28 (2021) 835–852.
- [52] D. Balarak, Z. Taheri, M.J. Shim, S.-M. Lee, C. Jeon, Adsorption kinetics and thermodynamics and equilibrium of ibuprofen from aqueous solutions by activated carbon prepared from *Lemna minor*, *Desal. Water Treat.*, 215 (2021) 183–193.
- [53] D. Balarak, A.H. Mahvi, M.J. Shim, S.-M. Lee, Adsorption of ciprofloxacin from aqueous solution onto synthesized NiO: isotherm, kinetic and thermodynamic studies, *Desal. Water Treat.*, 212 (2021) 390–400.
- [54] A.D. Khatibi, A.H. Mahvi, N. Mengelizadeh, D. Balarak, Adsorption-desorption of tetracycline onto molecularly imprinted polymer: isotherm, kinetics, and thermodynamics studies, *Desal. Water Treat.*, 230 (2021) 240–251.
- [55] M. Sillanpää, A.H. Mahvi, D. Balarak, A.D. Khatibi, Adsorption of Acid orange 7 dyes from aqueous solution using polypyrrole/nanosilica composite: experimental and modelling, *Int. J. Environ. Anal. Chem.*, (2021) 1855338, doi: 10.1080/03067319.2020.1855338.
- [56] T.J. Al-Musawi, N. Mengelizadeh, O. Al Rawi, D. Balarak, Capacity and modeling of Acid blue 113 dye adsorption onto chitosan magnetized by  $Fe_2O_3$  nanoparticles, *J. Polym. Environ.*, 30 (2022) 344–359, doi: 10.1007/s10924-021-02200-8.
- [57] T.J. Al-Musawi, N. Mengelizadeh, M. Taghavi, S. Mohebi, D. Balarak, Activated carbon derived from *Azolla filiculoides* fern: a high-adsorption-capacity adsorbent for residual ampicillin in pharmaceutical wastewater, *Biomass Convers. Biorefin.*, (2021), doi: 10.1007/s13399-021-01962-4.
- [58] A. Meshkinain, B. Davoud, Y. Nastaran, Optimization of nickel oxide nanoparticle synthesis through the sol-gel method for adsorption of Penicillin G, *Res. J. Chem. Environ.*, 25 (2021) 31–36.
- [59] H. Azarpira, Y. Mahdavi, O. Khaleghi, D. Balarak, Thermodynamic studies on the removal of metronidazole antibiotic by multi-walled carbon nanotubes, *Pharm. Lett.*, 8 (2016) 107–113.